Surface & Coatings Technology 203 (2008) 80–86

Contents lists available at ScienceDirect

Surface & Coatings Technology

journal homepage: www.elsevier.com/locate/surfcoat

Electrochemical evaluation of multilayer silica–metacrylate hybrid sol–gel coatings containing bioactive particles on surgical grade stainless steel

Josefina Ballarre [a,*], Damián A. López [a], Nataly C. Rosero [b], Alicia Durán [b], Mario Aparicio [b], Silvia M. Ceré [a]

[a] INTEMA, Universidad Nacional del Mar del Plata-CONICET, Juan B. Justo 4302, 7600 Mar del Plata, Argentina
[b] Instituto de Cerámica y Vidrio (CSIC), Campus de Cantoblanco, 28049 Madrid, Spain

ARTICLE INFO

Article history:
Received 18 February 2008
Accepted in revised form 2 August 2008
Available online 9 August 2008

Keywords:
Stainless steel
Coatings
Sol–gel
Bioactivity
Corrosion

ABSTRACT

Metallic materials are the most used materials as orthopaedic or dental implants because of their excellent mechanical properties. However they are not able to create a natural bonding with the mineralized bone and occasionally suffer localized corrosion. This work describes the electrochemical behaviour of a system of coatings with the addition of bioactive particles of the system SiO_2–CaO–P_2O_5, that enhance the abilities of the implant to make an union with the existing bone and to resist the extreme environment that are exposed to. The coatings were obtain from two kind of sols that were made by sol–gel process: one, using tetraethoxysilane (TEOS) and methyl triethoxysilane (MTES) as precursors, and the other using hydroxyethyl methacylate (HEMA), tetraethoxysilane (TEOS) and 3-methacryloxypropyl-trimethoxysilane (γMPS) [TMH] as precursor. Coatings were made in two layers. The inner layer was prepared either using TEOS and MTES (that had already shown good anticorrosion properties), or TMH. The top layer was made with TMH with the addition of 10% in weight of small (diameter less than 20 μm) or big (more than 20 μm) bioactive particles. The samples were tested in vitro by polarization curves and electrochemical impedance spectroscopy (EIS) assays. The samples with the two kind of coatings seem to have a protective behaviour after 30 days of immersion due to the compact TEOS–MTES inner layer. The big particles placed in the outer layer showed a dissolution rate similar to the rate of deposition of the amorphous hydroxyapatite (aHAp) at the surface, blocking the entrance of the electrolyte, avoiding it to reach the substrate. The TMH coatings with small particles present a similar behaviour to the naked material, allowing the electrolyte to reach the metal. The dual coating with this kind of particles has similar characteristics, with a "sponge-like" behaviour, and the inner coating probably develops flaws due to the fast dissolution of the small particles placed in the upper layer.

1. Introduction

The most common causes of failure of an orthopaedic or dental implant are the biological incompatibility or degradation of the piece. Metals are most commonly used materials that could be used due to for their mechanical properties [1–3], but the release of metallic particles due to wear or chemical degradation that could finally end in the removal of the implant [4,5]. Besides, most metals are not able to create a natural union with the mineralized bone. One way to improve the ion release is coating the metallic implant with a protective layer, which could be functionalized with the addition of bioactive particles to the films. Therefore the coating acts as a barrier avoiding the release of metal ions and it can make a bonding with the old bone by the formation of hydroxyapatite (HAp). Many coatings are used to improve the performance of metallic prosthesis, and one that shows biocompatibility is the silica based type with silane precursors [6,7].

The attainments of films by the sol–gel process have been successfully used on stainless steel, silver and aluminium; and have improved the oxidation and corrosion resistance of those metals [8,9]. It is possible to replace some inorganic components for organic ones, giving more plasticity to the structure [10,11] leading to a better adaptability to the substrate surface. Also this systems have the possibility of adding particles to the coating, reinforcing or functionalizing them for several proposes. The addition of bioactive particles and the dissolution and re-deposition of inorganic compounds of the apatite family, have been studied [12–16] as an attempt to provide the basic metal, a bone-like formation and adhesion to the existing structure. Methacrylate–silica based sol–gel films could also be an option to simulate the open structure of collagen fibers in new uncalciffied bone, for being the polymer structure less dense and more open than other hybrid coatings, and for having a biommimetic behaviour if they are correctly functionalized [17].

The electrochemical essays as electrochemical impedance spectroscopy (EIS) bring a non destructive way to analyze the life in service of the materials under study, giving a first approach to the knowledge of

* Corresponding author.
E-mail address: jballarre@fi.mdp.edu.ar (J. Ballarre).

0257-8972/$ – see front matter © 2008 Elsevier B.V. All rights reserved.
doi:10.1016/j.surfcoat.2008.08.005

the protective characteristics of the film and the deposited HAp layer with time [18–20].

The objective of this work is to analyze the electrochemical properties of a hybrid organic–inorganic coating on AISI 316L stainless steel with the inclusion of bioactive glass–ceramic particles of different size diameter.

2. Experimental

2.1. Substrates

Flat samples of stainless steel AISI 316L (Atlantic Stainless Co. Inc., composition: C 0.03% max, Mn 2% max, Si 1% max, P 0.045% max, S 0.03% max, Ni 10–14%, Cr 16–18%, Mo 2–3%) of 2×1 cm^2 area were used as substrates. They were sequentially cleaned with a soap solution, isopropylic alcohol and ultrasonic bath before the application of the coating.

2.2. Sol–gel sol

Two kinds of sols were used for the coatings: 1) TEOS (tetraethoxysilane)–MTES (methyltriethoxysilane), 2) TMH (TEOS (tetraethoxysilane)-γMPS (3-methacrylopropyl trimethoxysilane)-HEMA (2-hydroxyethyl methacrylate)). The TEOS–MTES sol was prepared by acid catalysis method in one stage, using TEOS (ABCR), and MTES (ABCR) as silica precursors; absolute ethanol as solvent and 0.1 M nitric and acetic acids as catalysts. The water was incorporated from the nitric acid solution in stoichiometric ratio. The molar ratio of TEOS/MTES was 40:60. All the reagents were stirred at 40 °C during 3 h obtaining a transparent sol (pH = 1–2, viscosity = 2.6 mPa s). The TEOS (ABCR)-γMPS (Dow Corning)-HEMA (Aldrich) (TMH) sol was made in a two steps procedure using 0.1 M nitric acid and isopropylic alcohol. The solution, containing 40 g l^{-1} of SiO_2, was stirred at 65 °C for 36 h in glycerine bath. Detailed preparation of the sol is given elsewhere [21].

2.3. Glass–ceramic particles

The glass–ceramic particles were made from a precursor glass of the system SiO_2–P_2O_5–CaO. The precursors used were silica sand, calcium carbonate (Aldrich) and orthophosphoric acid (Aldrich). The ratio of each one was calculated in order to obtain the concentration of CaO of 47.29%, SiO_2 35.69% and P_2O_5 17.01% in weight in the final glass. The mixture was fused in a platinum crucible at 1600 °C in air atmosphere, and then quenched in water. The thermal treatment was made at 1050 °C for 2 h in an electric furnace with the aim of obtaining apatite and wollastonite as crystalline phases. The glass–ceramic obtained was milled in an agate planetary mill (Frizsth Pulverisette, Germany), using a speed of rotation of 1500 rpm for 4 h. After this process, the particles were screened with Tyler screens (nrs. 270, 325 and 600) to obtain different diameter size distribution of bioactive particles. Two particle size distributions were used: a) "small particles" (s.p.) for particles with diameter less than 20 μm; and b) "big particles" (b.p.) for particles with diameter bigger than 20 μm but smaller than 45 μm.

2.4. Suspensions

The particle suspensions were prepared by the addition of 10% in weight of particles with respect to the solution. The suspensions were stirred by a high shear mixing in a rotor–stator agitator (Silverson L2R, UK) during 6 min. After the first 3 min, approximately 15% by weight of solids of Triton X 114 Surfactant (Dow Corning) was added as dispersant in the glass–ceramic containing suspensions. The Triton

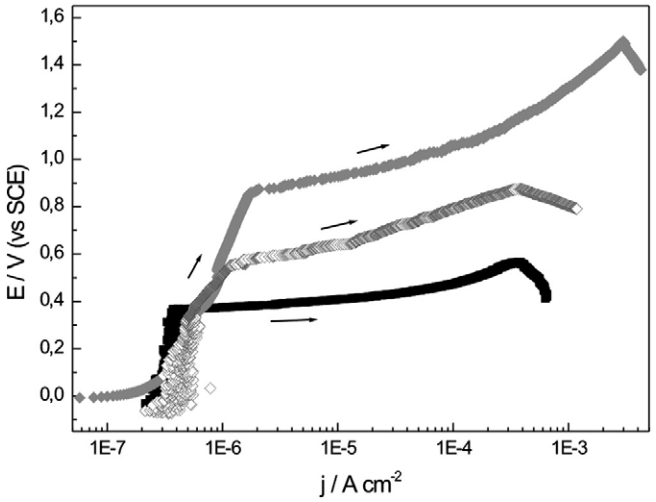

Fig. 2. Potentiodynamic polarization curve of the TEOS–MTES + TMH coating containing small particles after 1 (◆) and 30 (◇) days of immersion in SBF and their comparison with the bare alloy (■).

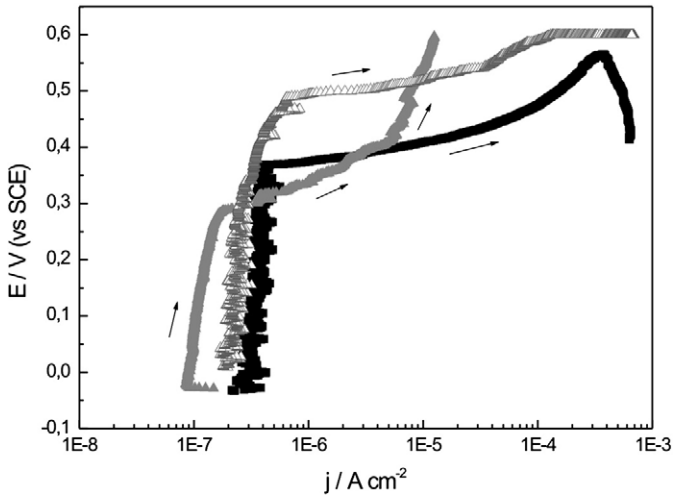

Fig. 1. Potentiodynamic polarization curve of the TMH coating containing big particles after 1 (▲) and 30 (Δ) days of immersion in SBF and their comparison with the bare alloy (■).

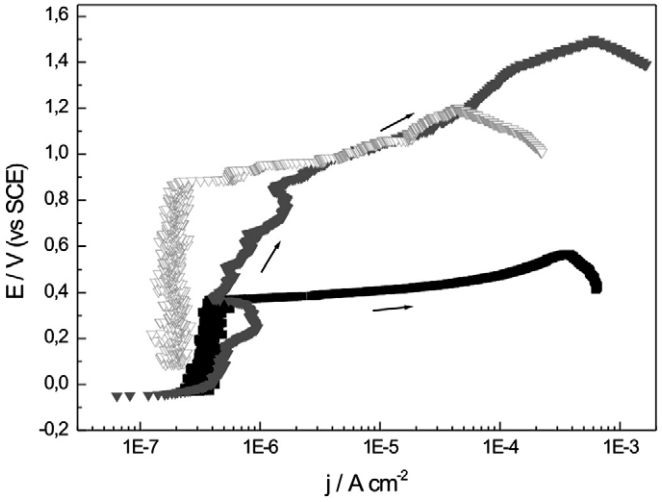

Fig. 3. Potentiodynamic polarization curve of the TEOS–MTES / TMH coating containing big particles after 1 (▼) and 30 (▽) days of immersion in SBF, and their comparison with the bare alloy (■).

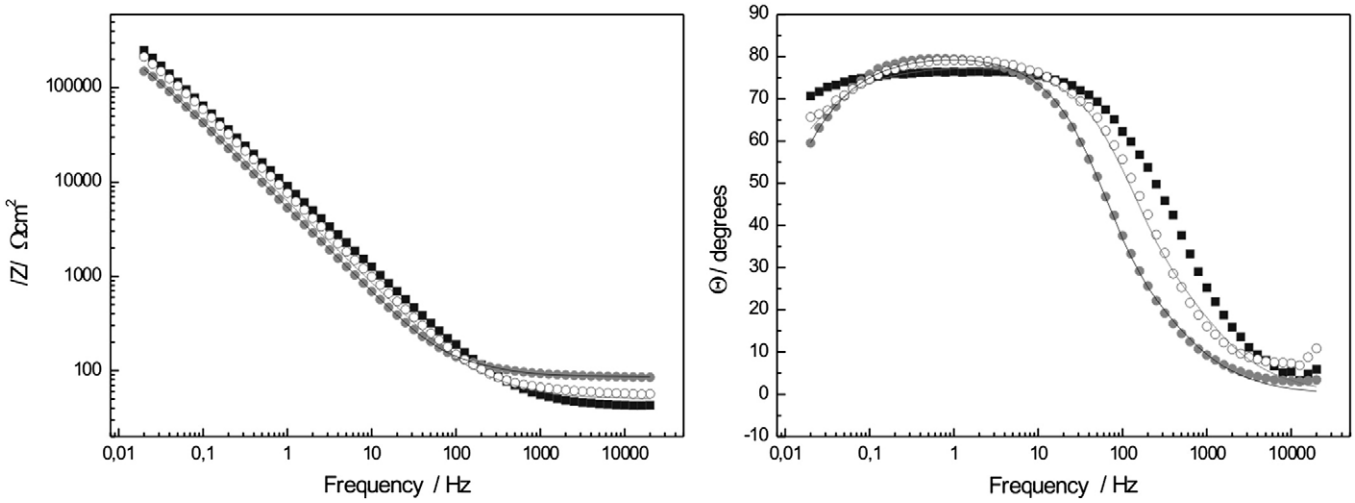

Fig. 4. Bode plots for the TMH coating containing small particles after 1 (●) and 30 (o) days of immersion in SBF and their comparison with the bare alloy (■).

works as a surfactant that adsorbs on the surface of the glass–ceramic particles, creating an electrostatic repulsion between the particles and avoiding segregation [22].

2.5. Coatings

Coatings were obtained by the dip-coating technique at room temperature, and withdrawn at 25 cm min^{-1}. Experimental details are shown elsewhere [23,24].The different types of coatings that were used in this work are the following:

a) Two layers of TMH without thermal treatment in between followed by a third layer of TMH containing a suspension of 10% weigh in volume of bioactive particles (some samples with small particles and some with big ones).
b) A single layer of TEOS–MTES treated at 450 °C during 30 min, and then a second layer deposited on top of if consisting in two layers of TMH hybrid (without thermal treatment in between), followed by a third layer of TMH containing a suspension of 10% weigh in volume of bioactive particles (either small or big particles).

Finally all kind of coatings were heat treated at 150 °C for 60 min in air atmosphere.

The coating thickness were measured on glass samples by using a profilometer (Talystep, Taylor-Hobson, UK) on a scratch made immediately after deposition. The average of three measurements was taken as the final value.

2.6. Electrochemical analysis

A simulated body fluid (SBF) solution was used as electrolyte in all the experiments. SBF was prepared with the following chemical composition [25]: NaCl (8.053 g l^{-1}), KCl (0.224 g l^{-1}), $CaCl_2$ (0.278 g l^{-1}), $MgCl_2{\cdot}6H_2O$ (0.305 g l^{-1}), K_2HPO_4 (0.174 g l^{-1}), $NaHCO_3$ (0.353 g l^{-1}), $(CH_2OH)_3\,CNH_2$ (6.057 g l^{-1}). Concentrated hydrochloric acid (HCl) was added to adjust the pH to 7.25 ± 0.05.

The samples were immersed in SBF for 24 h and 30 days, and sealed at 37 °C in a sterilized furnace until the tests were done. All test were performed at both periods of time.

Electrochemical assays were carried out in a Solartron 128B electrochemical unit with a conventional three electrode cell. The reference electrode was a saturated calomel electrode (SCE, Radiometer Copenhagen), a platinum wire as a counter electrode and the stainless steel, either bare or coated as working electrode.

Potentiodynamic polarization curves were conducted from the corrosion potential (E_{corr}) to 1 V and backwards, or up to a maximum current density of 0.001 A cm^{-2}, at a sweep rate of 0.002 V s^{-1}. Electrochemical impedance spectroscopy (EIS) tests were registered at the E_{corr} with an amplitude of 0.005 V rms sweeping frequencies from

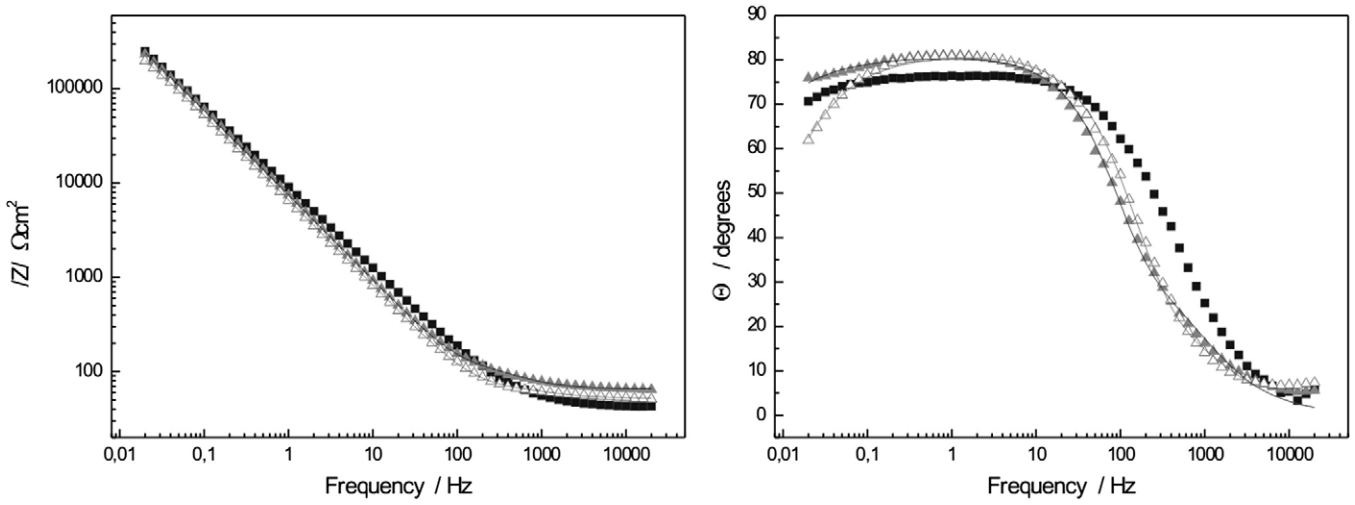

Fig. 5. Bode plots for the TMH coating containing big particles after 1 (▲) and 30 (Δ) days of immersion in SBF and their comparison with the bare alloy (■).

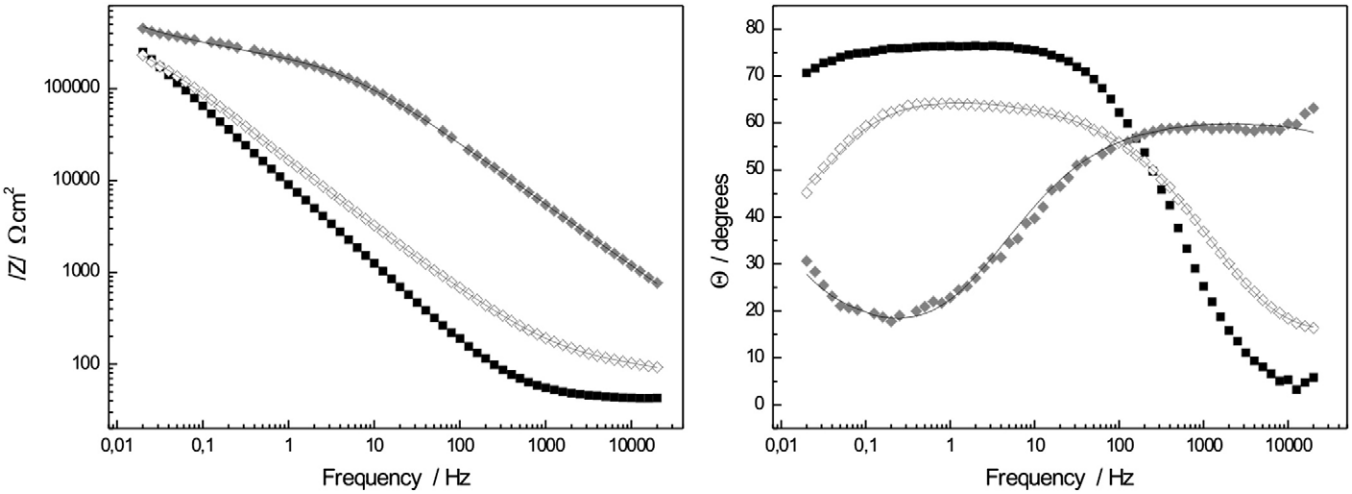

Fig. 6. Bode plots for the TEOS–MTES+TMH coating containing small particles after 1 (◆) and 30 (◇) days of immersion in SBF and their comparison with the bare alloy (■).

20,000 to 0.02 Hz. Impedance data fitting was performed using Zplot Windows software.

Scanning Electron Microscopy (SEM, Phillips XL 30) images were taken to the surface of the samples after 24 h and 30 days of immersion in SBF.

3. Results and discussion

Potentiodynamic curves of the TMH samples either with small (not shown) or big particles (Fig. 1) have a similar behaviour after 30 days of immersion in SBF. Current density around corrosion potential and pitting potential (E_{pit}) for the coated samples are almost the same (2×10^{-7} A cm^{-2} and 0.4 V) than for the naked material (substrate, AISI 316 L), showing no improvement in the coating protective behaviour. Only a slight decrease in the current density of the TMH with big particles coated sample after 30 days of immersion is observed.

The dual TEOS–MTES/TMH coating containing small particles (Fig. 2) shows similar current density than the bare alloy although the breakdown potential shifts anodic for the coated material.

Fig. 3 shows TEOS–MTES/TMH coating containing big particles. Although current densities remained unaltered after 24 h of immersion when compared with bare alloy, after 30 days of immersion the curve shifts left showing a decay in current density.

The dual coatings with TEOS–MTES and TMH present larger breakdown potential than the TMH ones because of the presence of an inner more inorganic protective film (TEOS–MTES) [11,26,27]. The electrochemical behaviour of those coatings without particles was studied in previous work [21].

Electrochemical impedance spectroscopy (EIS) tests on TMH coated samples containing both size particles do not reveal remarkable differences between them and with the uncoated (bare) steel (Figs. 4 and 5). In both cases either with small or big particles, and after 24 h and 30 days of immersion, there was no clear maximum showed in the phase angle vs. frequency Bode plot. The high angle (near 80°) from 0.1 to 30 Hz reveals a capacitive behaviour, showing an impedance response similar to the metallic substrate. The decay in phase angle between 10,000 and 10 Hz in TMH coated samples could be associated with a diffusive-controlled response. In that frequency range, the samples with 30 days of immersion have a small increase in phase angle indicating that the film (with small or big particles) has less conductive paths than the ones with 24 h of immersion. In the samples with TMH coating and big particles (Fig. 5) this behaviour is very similar for 24 h and 30 days.

Samples coated with dual coating system (TEOS–MTES/TMH) containing small particles (Fig. 6) showed two time constants, noticed in the change of slope in /Z/ vs. frequency plot at approximately 10 Hz. Also, the presence of two time constants is insinuated in the phase angle vs. frequency plot, where the positions of the peaks seem to be very apart from each other. After 30 days of immersion there is an

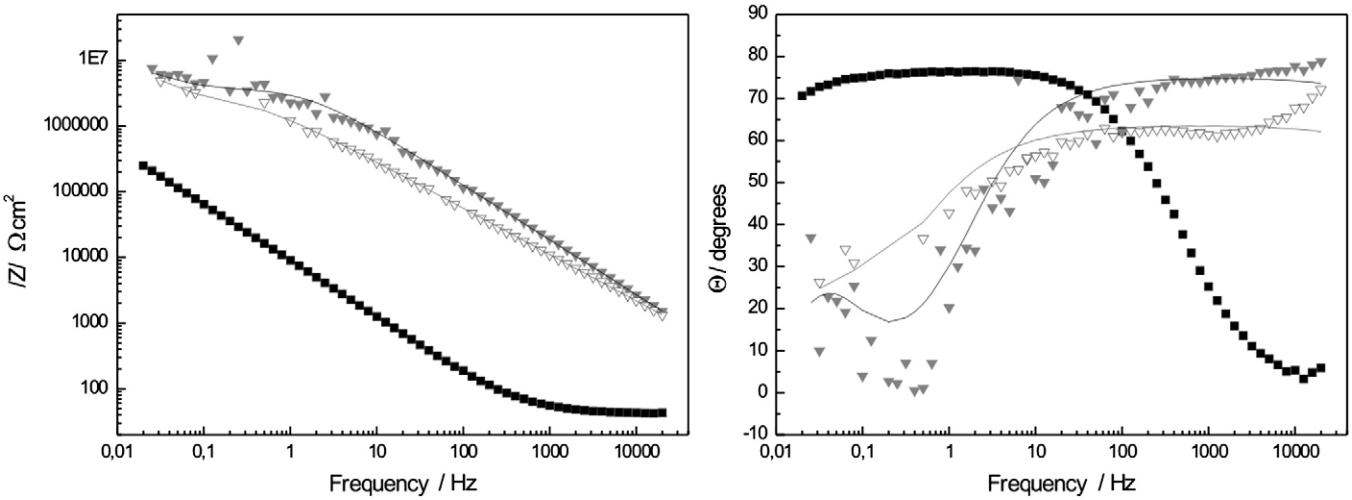

Fig. 7. Bode plots for the TEOS–MTES+TMH coating containing big particles after 1 (▼) and 30 (▽) days of immersion in SBF and their comparison with the bare alloy (■).

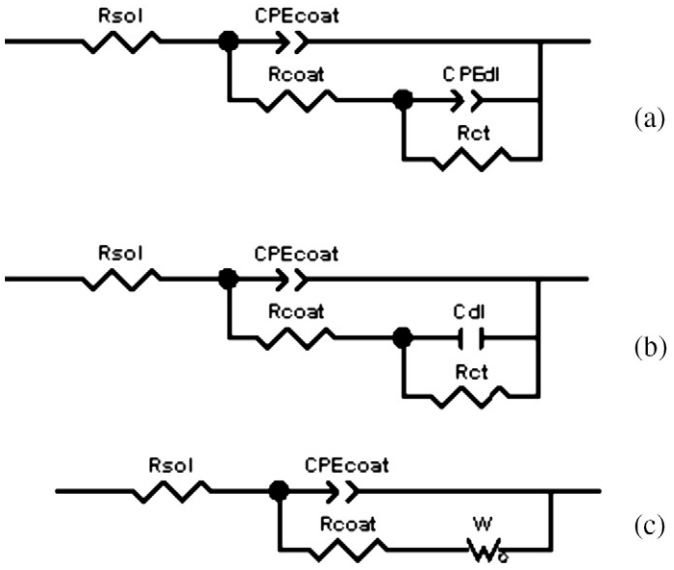

Fig. 8. Equivalent electric circuits employed to model the impedance data of the different coatings after 1 and 30 days of immersion in SBF.

increase in the phase angle value in the middle range of frequencies, showing two close time constants.

Fig. 7 introduces EIS Bode plots for TEOS–MTES/TMH coatings with big particles. The total resistance of the system is higher for the dual coating with particles for both times of immersion than for the bare steel, at very low frequencies. The phase angle vs. frequency plots shows some deterioration for the coated samples with time, and a little capacitive behaviour at high frequencies.

In previous work [21], it has been proposed that TMH coating without addition of bioactive particles shows a "porous layer" behaviour: the coating allows the entrance of the electrolyte to the coating reaching the metallic substrate. This behaviour was modelled with an equivalent electric circuit (Fig. 8a), where a constant phase element (CPE) instead of a capacitor was used, as the phase angle capacitor was different from −90°. According, C_{coat} and C_{dl} represent the pseudocapacitance of the coating and double layer respectively and n is the coefficient related with the system homogeneity. R_s and R_{coat} represent the solution and coating resistance. The R_{ct} represents the electrochemical double layer (or charge transference) resistance.

The TMH coated samples with the addition of small or big particles for both immersion times (1 and 30 days) in simulated body fluid show a similar EIS response. They can be electrically modelled by the circuit showed in Fig. 8b, which contains an ideal capacitor instead of a constant phase element (the n parameter equal to 1). The fitting results are shown in Table 1. The behaviour observed is similar for the samples with big particles than for the ones with small ones, with a poor electrical response of the coating and similar capacitance of the double layer. The coating resistance is low and similar to the solution resistance. The capacitance of the double layer remains almost constant for all the studied immersion times. The fact that this system was modelled with an ideal capacitor could be related with the presence of the smooth surfaces created by the fine particles and the aHAp that is thought to be deposited at the surface. In previous work, the percentage of the surface covered by the particles was analyzed, and it was found to be less than 10% at 24 h, reaching a 53% of coverage after 30 days of immersion [28].

After 1 day of immersion, the samples with big particles showed higher resistance to the charge transfer than the samples with small particles at all the immersion times (Table 1). It can be explained assuming a slow rate of dissolution of the big particles compared with the small ones, allowing the deposition of aHAp at a similar rate. After 30 days, the total resistance of the system decays, reaching the value of the TMH coating with small particles.

The dual hybrid coating TEOS–MTES/TMH with the addition of small particles can be modelled with an equivalent circuit (Fig. 8c) with a Warburg element. The Warburg impedance is used to model increasing ionic conductivity due to corrosion processes occurring inside the pores and increasing diffusivity into them. When the thickness of the film is little, low frequencies will penetrate along all the thickness creating a finite length Warburg element [29,30]:

$$Z_W = \frac{R_{DO}}{(jT\omega)^n}\tan h(jT\omega)^n \quad (1)$$

In this equation R_{DO} is associated with a solid state diffusion and T is related to diffusion coefficient and pore length.

The TEOS–MTES/TMH coating with small particles after 1 day of immersion present a total resistance of the system higher than the ones found for the TMH coating with the same kind of particles (Fig. 6). Nevertheless after 30 days of immersion in SBF, it shows a drastic drop in R_{coat} value due to the dissolution of the particles, leaving cracked zones in the surrounding area. This fact is thought to be necessary step for the dissolution of calcium phosphate particles and the deposition of HAp [26,31]. The rate of dissolution of the particles needs to be similar to the rate of deposition of the aHAp, to reach a steady state. In the present case, the rate of particle dissolution seems to be lower and therefore the inner coating suffers a breaking process, creating preferential paths and allowing the electrolyte to reach the metallic substrate.

Other sign of particle dissolution and further deposition of the calcium phosphate compounds is the raise in the coating capacitance (C_{coat}). According to Eq. (2), C_{coat} will raise due to the enlargement of the superficial area (A) due to the deposition of HAp compounds, and the change in the permittivity (ε) caused by the deposition of these compounds on cracks and pores present in coating or by the entrance of the electrolyte in them.

$$C_{coat} = \frac{\varepsilon\ \varepsilon_o A}{d} \quad (2)$$

The coatings of TEOS–MTES/TMH containing big particles showed a slight deterioration tendency after 30 days of immersion in SBF,

Table 1
Fitting parameters using the equivalent circuits shown in Fig. 8

	R_s /Ω cm^2	R_{coat} /Ω cm^2	CPE_{coat}		W_o			C_{dl} /Ω^{-1} cm^{-2} s^n	R_{ct}/Ω cm^2
			C_{coat}/Ω^{-1} cm^{-2}s^n	n	R_{DO}/Ω cm^2	T/s	n		
TMH s.p. 01	86.11	174.4	2.98E−05	0.873				5.96E−06	4.42E+05
TMH s.p. 30	50.45	160	2.88E−05	0.845				3.76E−06	6.55E+05
TMH b.p. 01	65.16	135.5	1.97E−05	0.86				6.15E−06	2.72E+06
TMH b.p. 30	52.01	49.48	2.21E−05	0.867				6.63E−06	6.42E+05
T-M/TMH s.p. 01	43	2.46E+05	4.74E−07	0.676	6.05E+05	60.46	0.5		
T-M/TMH s.p. 30	43	101.2	9.02E−06	0.608	2.39E+06	44.69	0.77		
T-M/TMH b.p. 01	42	3.95E+06	3.65E−08	0.83				1.36E−06	4.33E+06
T-M/TMH b.p. 30	42	7.20E+06	8.32E−08	0.76	1.16E+08	99.05	0.973		

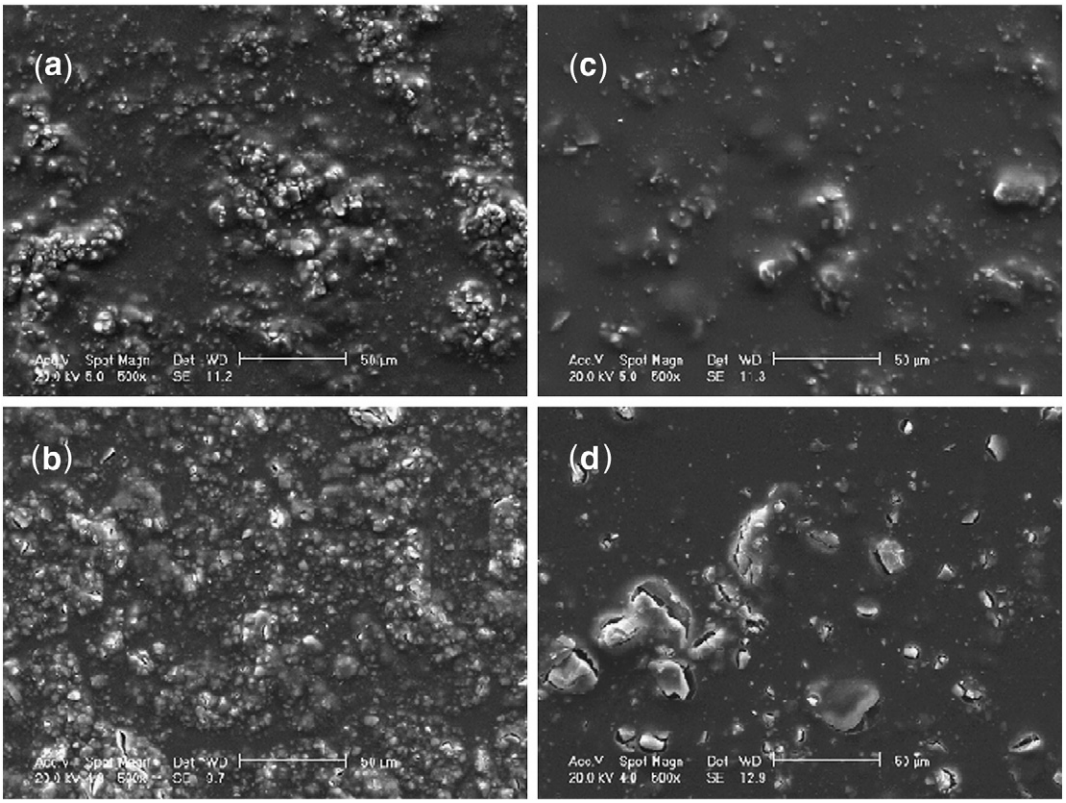

Fig. 9. Scanning Electron Microscopy of TEOS–MTES/TMH coated samples with small particles after 1 (a) and 30 days (b) of immersion, and samples with big particles after 1 (c) and 30 days (d) of immersion in SBF at 37 °C.

showing a similar behaviour with the TMH coatings with the same kind of particles. This big particles have a slower rate of dissolution than the small ones because of the less superficial and reactive exposed area, and the rhythm of crack formation is comparable with the rate of deposition of the amorphous HAp, as it was sawn with the TMH coatings, delaying the deterioration rate of the coating. This difference in dissolution rate can be seen in SEM images (Fig. 9). The photographs show TEOS–MTES/TMH coatings with small particles with 1 and 30 days of immersion in SBF (Fig. 9a and b), and the same dual coatings with big particles in the upper layer, after 1 and 30 days of immersion (Fig. 9c and d). When the TEOS–MTES/TMH coating contains big particles, the film behaves as layer with in-homogeneities or defects after 24 h of immersion in SBF. The electric behaviour could be simulated again with the incorporation of a Warburg element, adding to the model the presence of deposits over the flaws or the pores. This fact can be sustained with a decrease in the current density after 30 days (Fig. 3) in the zone of the corrosion potential at the potentiodynamic tests. The R_{coat} has a pronounced increment in his value comparing the dual coatings with big and small particles, sustaining the fact that the dissolution rate of the small particles is bigger that the one of the big ones, leading to the formation of cracks and pores unfilled with amorphous hydroxyapatite recently formed.

4. Conclusions

Two-layer hybrid sol–gel coatings on stainless steel AISI 316L were made using TEOS and MTES, and TEOS, MPS and HEMA [TMH]. The outer layer of the two systems was TMH and it was functionalized with the addition of two different size bioactive particles.

The samples with the dual coating (TEOS–MTES/TMH) seem to have a better corrosion resistance after 30 days of immersion when compared with double layer TMH coatings because of the higher densification degree of the more inorganic TEOS–MTES inner layer.

The TMH coatings with small particles present a similar behaviour to the naked material, allowing the electrolyte to reach the metal. The dual coating (TEOS–MTES/TMH) with this kind of particles has similar characteristics, showing a “sponge-like” behaviour and probably develops flaws in the inner coatings due to the fast dissolution of the small particles placed in the upper layer.

The big size particles placed in the outer layer have a slower dissolution rate than the small ones. This fact can be attributed to the less superficial and reactive exposed area of the big particles. The rate of fissure formation at the surrounding of the particle is thought to be comparable with the deposition rate of aHAp, delaying the deterioration of the coatings.

Acknowledgements

The authors would like to thanks the National Research Council of Argentina (CONICET), Spanish Project MAT2006-4375, for the financial support.

References

[1] K.S. Katti, Biomaterials in total joint replacement, Colloids Surf. B, Biointerfaces 39 (2004) 133.
[2] J.B. Park, Biomaterials Science and Engineering, Plenum Press, New York, 1984.
[3] J.V. Sloten, L. Labey, R.V. Audekercke, G. Van der Perre, Biomaterials 19 (16) (1998) 1455.
[4] Y. Okazaki, E. Goloh, T. Manabe, K. Kobayashi, Biomaterials 25 (2004) 5913.
[5] J. Woodman, J. Black, D. Nunamaker, J. Biomed. Materi. Res. 17 (1983) 655.
[6] A. Kros, M. Gerritsen, V.S.I. Sprakel, N.A.J.M. Sommerdijk, J.A. Jansen, R.J.M. Nolte, Sens. Actuators, B, Chem. 81 (2001) 68.
[7] T.P. Chou, C. Chandrasekaran, S.J. Limmer, S. Seraji, Y. Wu, M.J. Forbess, C. Nguyen, G.Z. Cao, J. Non-Cryst. Solids 290 (2001) 153.
[8] O. de Sanctis, L. Gomez, N. Pellegri, C. Parodi, A. Marajofsky, A. Durán, J. Non-Cryst. Solids 121 (1990) 338.
[9] O. de Sanctis, L. Gomez, N. Pellegri, A. Durán, Surf. Coat. Technol. 70 (2–3) (1995) 251.

[10] P.G. Galliano, J.J. de Damborenea, M.J. Pascual, A. Durán, J. Sol–Gel Sci.Technol. 13 (1998) 723.
[11] L.E. Amato, D.A. López, P.G. Galliano, S.M. Ceré, Mater. Lett. 59 (2005) 2026.
[12] P.N. De Aza, Z.B. Lulinska, C. Santos, F. Guitian, S. De Aza, Biomaterials 24 (2003) 1437.
[13] A. Oyane, K. Nakanishi, H.M. Kim, F. Miyaji, T. Kokubo, N. Soga, T. Nakamuro, Biomaterials 20 (1999) 79.
[14] C. Ohtusuki, T. Kokubo, T. Yamamuro, J. Non-Cryst. Solids 143 (1992) 84.
[15] O. Peitl, E. Dutra Zanotto, L.L. Hench, J. Non-Cryst. Solids 292 (2001) 115.
[16] T. Kokubo, H. Kushitani, C. Ohtsuki, S. Sakka, T. Yamamuro, J. Mater. Sci., Mater. Med. 3 (1992) 79.
[17] K. Prashantha, B.J. Rashmi, T.V. Venkatesha, Joong-Hee Lee, Spectrochim. Acta, Part A 65 (2006) 340.
[18] B.R. Hinderliter, S.G. Croll, D.E. Tallman, Q. Su, G.P. Bierwagen, Electrochim. Acta 51 (2006) 4505.
[19] J. Gallardo, A. Durán, J.J. de Damborenea, Corros. Sci. 46 (2004) 795.
[20] K.J. Bundy, J. Dillard, R. Luedemann, Biomaterials 14 (7) (1993) 529.
[21] D.A. López, N.C. Rosero-Navarro, J. Ballarre, A. Durán, M. Aparicio, S. Ceré, Surf. Coat. Technol. 202 (10) (2008) 2194.
[22] C. García, A. Durán, R. Moreno, J. Sol–Gel Sci. Technol. 34 (2005) 1.
[23] P.C. Innocenzi, M. Guglielmi, M. Gobbin, P. Colombo, J. Eur. Ceram. Soc. 10 (1992) 431.
[24] M. Guglielmi, S. Zenezini, J. Non-Cryst. Solids 121 (1990) 303.
[25] T. Kokubo, H. Kushiani, S. Sakka, T. Kitsugi, T. Yamamuro, J. Biomed. Mater. Res. 24 (1990) 721.
[26] C. García, S. Ceré, A. Durán, J. Non-Cryst. Solids 348 (15) (2004) 218.
[27] J. Gallardo, P. Galliano, A. Durán, J. Sol–Gel Sci. Technol. 21 (2001) 65.
[28] J. Ballarre, D.A. López, W. Schreiner, A. Durán, S. Ceré, Appl. Surf. Sci. 253 (2007) 7260.
[29] N.D. Cogger, N.J. Evans, An introduction to Electrochemical Impedance Measurements, Technical Report No. 6, Part: BTR006, vol. 5, Solartron Limited, UK, 1999.
[30] F. Mansfeld, Analysis and interpretation os EIS data for metals and alloys, Technical Report N°26, Part: BTR026, AB, Solartron Limited, UK, 1999.
[31] C. García, S. Ceré, A. Durán, J. Non-Cryst. Solids 352 (32–35) (2006) 3488.